

Experimental study of river morphology downstream of the inclined and vertical grade control structures

Seyed Mohamad Mahdi Shariati¹
Mehdi Hamidi^{*1}

Abstract

Grade control structure (GCS) can be used to reduce erosion in river beds. They decrease the river bed scour by changing the flow regime and reducing its velocity. It is required to maintain the stability of these structures against the scour hole that generates downstream of them, so investigating the scour hole characteristics downstream of the GCS is inevitable. In the present research, the equilibrium scour holes downstream of GCS were investigated under three discharges ($q=0.00467, 0.00583, 0.00700 \text{ m}^3/\text{s.m}$) and two different sedimentation conditions ($d_{50}=0.082, 1.6 \text{ mm}$). The results show that in the constant GCS geometry and finer sediment, the maximum scour depth (d_s) and maximum scour hole length (l_s) increase. In the same sedimentary conditions and different geometry, when the slope of the GCS downstream face varied from 90° to 60° , d_s increases, but l_s decreases. Also, the hydraulic jump forms on the scour hole at high flow intensity, which has an essential influence on the geometry of the equilibrium scour hole. Comparison of d_s/H_c between the present study and Ben Meftah and Mossa (2020) has $R_2=0.891$ and $RE=10.66\%$, which reveals acceptable compatibility between the present study results and previous ones.

Keywords: Experimental model, Grade control structure, Maximum scour depth, River engineering, Sediment transport.

Received: 18 June 2024; Accepted: 30 July 2024

1. Introduction

One problem of hydraulic structures and river engineering is the erosion of the sedimentary beds and sidewalls of rivers or irrigation channels, caused by the interaction of water flow and sediment [1]. Among the countermeasures to reduce this phenomenon, using bed stabilization structures are common, which are divided into different types. One of the most important of these structures is the inclined and vertical grade control structures (GCS). The performance of these structures is according to the conservation mass law; the water depth behind these structures increases, and as a result, the water flow velocity decreases. It is understandable that the higher the flow velocity, the more intensive scour occurs. In fact, by changing the flow regime, the erosion in the sedimentary bed can be reduced to some extent.

* E-mail: hamidi@nit.ac.ir (Corresponding Author)

¹ Faculty of Civil Engineering, Babol Noshirvani University of Technology, Babol, Mazandaran, Iran.



The installation of GCS has become an ideal choice for river engineers to reduce sediment bed erosion because these structures are eco-friendly structures that help river restoration and improve aquatic life [2-4]. The expansion of the scour hole downstream of GCS may cause damage to it [5]. Therefore, studying the development of scour downstream of GCS for their management and safety is necessary. Despite using numerical methods to predict the longitudinal profile of the scour hole around hydraulic structures, experimental techniques, and objective observations still provide researchers with more reliable results. In the following, some of the most important results of the previous experimental studies have been investigated.

In 1991, Bormann and Julien studied the GCS with the different downstream face slopes experimentally. They observed that the maximum scour depth (d_s) downstream of the vertical GCS is dependent on the flow velocity [6]. In 1998, Mossa studied the longitudinal patterns of the scour hole formed downstream of GCS and realized that some of the results obtained (maximum scour depth) were not consistent with the previous technical literature formulas [7]. Therefore, he performed a proper dimensional analysis for better results [7]. Lenzi et al. (2003) performed a comprehensive field and experimental study on the depth of downstream scour holes of seventy-three GCS of the bed sill type in 6 mountainous rivers in the Italian Alps [8]. Their research indicated that the differences in sediment particles in terms of size and lithology have a minor influence on defining the size of the scour hole. The maximum measured scour depth was well calculated by a semi-empirical relation proposed by the experimental data, which showed an average relative error of 0.13 [8]. Marion et al. (2004) evaluated the distance of bed sills from each other and sediment granularity [9]. They found a new relationship for high-gradient flows, i.e., a slope greater than 0.4, and sediment size, which is significantly effective. They focused on the dimensions of the scour hole, which is included in their prediction formula [9]. In 2004, D'Agostino and Ferro investigated the scour hole downstream of a weir [10]. The results of their experiments indicated that the ratio of flow head to weir height can describe the measurements of the scour depth in, both large and small scales. The parameters of the longitudinal scour profiles were calculated more accurately than the scour depth. They seemed to be more affected by the coarse particles of the sedimentary bed [10]. Pagliara and Palermo (2013) investigated the scour hole downstream of rock grade control structures and stepped gabion weirs and concluded that these structures have a significant effect on the flow regime and river morphology [11]. As a result, this flow regime in developing scour holes is effective, and hydraulic jump affects sediment transport significantly [11]. Pagliara and Kurdistani (2014) investigated W and V weirs [12]. They found that the foremost effective parameters for predicting the maximum scour depth and length include the densimetric Froude number, the weir height, and the water drop height. It was observed that the d_s downstream of the W-shaped weir is greater than that of the V-shaped weir [12]. Shafai-Bejestan et al. (2016) evaluated the effects of upward water seepage on d_s [5]. They concluded that, in general, upward seepage reduces the downward velocity close to the bed, which reduces d_s [5]. Rajaei et al. (2018) studied the trapezoidal and rectangular labyrinth weirs [13]. They found that labyrinth weirs have a significant influence on decreasing d_s downstream of GCS, and the scour depth downstream was reduced by 19% in the trapezoidal weir and 10% in the rectangular weir compared to the linear weir [13]. Di Nardi et al. (2021) studied the ability to predict the scour evolution model based on the PTT method using a large data set related to GCS [14]. They figured out that PTT is a valid method for estimating scour development irrespective of the structural configuration and hydraulic conditions. It is unnecessary to provide limited hydraulic conditions to perform the experiments as in the previous studies [14]. The piano key weir (PKW) is a GCS with more hydraulic efficiency, compared to the labyrinth weir [15-16]. Lantz et al. (2022) evaluated the

evolution of scour downstream of the piano key weir [17]. They concluded that the hydraulic conditions, especially in the tailwater, have a significant effect on the equilibrium scour process, which ultimately leads to the scour depth more than the weir height. Khalili and Hamidi (2023) investigated the submerged hydraulic jump formed on the floor downstream of the sluice gate [18]. They observed that the average velocity at the end of the sediment bed is about 18% lower than at the beginning. Scouring occurs in submerged vertical jets downstream of some grade-control structures [19]. Guguloth et al. (2024) predicted scour hole depths for static and dynamic conditions as a result of submerged circular vertical jets with AI models and received accurate results [20].

Some studies show that secondary currents also play an essential role in developing scour holes in GCS. Ben Meftah et al. (2021) in an experimental study indicated that d_s downstream of GCS is formed closer to the sidewalls of the channel and is far from the channel's centerline [21].

It can be concluded by reviewing technical literature that the sedimentary conditions, the flow hydraulic conditions, and the geometry of GCS are the main factors on the longitudinal profile of the scour hole downstream of GCS. Although experimental studies have been performed on the scour downstream of vertical and inclined GCS, most of them are on GCS with an angle of 45° or less. Therefore, this study compared the longitudinal profiles of the scour hole downstream of GCS with 90° and 60° . Also, the effects of geometric changes in GCS and sediment granularity on the longitudinal profile of the scour hole were investigated, and the maximum depth (d_s) and length (l_s) of the scour hole were compared. Two laboratory models of vertical and inclined GCS have been used in the tests. The present study focused on the profile of scour hole development downstream of GCS in different sedimentary and geometry conditions in the same tailwater depth. Dimensional analysis has been provided by using the available equations from previous studies, and the experimental setup was presented based on it and previous data.

2. Materials and methods

2.1. Dimensional analysis

To obtain correct and reliable results each test requires appropriate dimensional analysis according to the scale of the experimental model. According to Noormohammadi et al. [22], the most critical parameters affecting the scour downstream of inclined GCS are the hydraulic conditions, the geometric conditions of the structure, the characteristics of the sedimentary bed, and the time of the scour process.

The physical model in the present study was similar to the study of Ben Meftah and Mossa (2020) [23]. Thus, for this research separate dimensional analyses were not applied and similar effective parameters were used. According to their study, due to the high-velocity gradient between the water inlet and the scour hole, a drag force is generated. If it is greater than the weight of the bed sediment particles, it leads to sediment transport and particle movement. The scouring process reaches an equilibrium condition when the non-cohesive sediment bed particles are not separated from the scour hole and are not transported downstream. In clear water conditions, an equilibrium condition in the scour process occurs when the geometry of the longitudinal profile of the scour hole downstream of the GCS does not change with time under steady flow conditions. Due to the turbulence in the flow, there is a possibility of changes in the final condition of the longitudinal scour patterns downstream of GCS. Based on Mason and Arumugam (1985) [24], these changes are minor and the theory of d_s is acceptable and consistent for the engineering design consideration. Ben Meftah and Mossa (2020) [23] presented Eq. (1) for the influential variables of the scour phenomenon.

$$d_s, l_s = f(d_{50}, H_c, H_t, g, q, Z_d, \lambda, \nu, \rho_s, \rho_w) \quad (1)$$

In Eq. (1), d_s is the maximum scour depth, l_s is the maximum length of the scour hole, d_{50} is the median sediment particle size, H_c is the depth of the water inlet jet or the flow critical depth, H_t is the tailwater depth, g is the acceleration of the earth's gravity, q is the flow discharge per unit width, Z_d is the level difference between the GCS crest and the primary sedimentary bed, λ is the angle between the downstream face of GCS and channel floor, ν is the kinematic viscosity of water, ρ_s is the density of sediment particles and ρ_w is the water density. The Eq. (1) can be substituted with dimensionless Eq. (2).

$$\frac{d_s}{H_c}, \frac{l_s}{H_c} = f\left(\frac{d_{50}}{H_c}, \frac{Z_d}{H_c}, \frac{H_t}{H_c}, \frac{1}{Fr_c^2}, \frac{1}{Re}, \lambda, \frac{\rho_s - \rho_w}{\rho_w}\right) \quad (2)$$

In Eq. (2), Fr_c and Re represent Froude's number on the end of the GCS crest and Reynolds number, respectively. In turbulent flow, the influence of Re on the scouring process can be neglected, so the final relation is written as follows.

$$\frac{d_s}{H_c}, \frac{l_s}{H_c} = f\left(\frac{Z_d}{H_c}, \frac{H_t}{H_c}, \lambda, \frac{q}{H_c \sqrt{(\Delta - 1)g} \cdot d_{50}} = Fr_d\right) \quad (3)$$

In Eq. (3), Fr_d presents the densimetric Froude number, which is written as $\frac{q}{H_c \sqrt{(\Delta - 1)g} \cdot d_{50}}$ and term Δ shows $\frac{\rho_s}{\rho_w}$.

Despite the studies that have been carried out on scouring and bed erosion downstream of GCS and available equations that have been obtained, predicting the geometry of the longitudinal profile scour hole in equilibrium conditions is still challenging. In different ranges of hydraulic conditions, different geometries of GCS, and sedimentary conditions, there are several equations, each limited to the dimensional analysis and characteristics of its laboratory conditions. According to Ben Meftah and Mossa (2020) [23], most available equations for GCS were derived from Mason and Arumugam (1985) equation [24], as Eq. (4).

$$d_s + H_t = K \frac{q^a \cdot H^b \cdot H_t^c}{g^e \cdot d_{50}^f} \quad (4)$$

H is the gap between the water head level and the tailwater depth, $K = 6.42 - 3.10H^{0.01}$, $a = 0.60 - \frac{H}{300}$, $b = 0.15 - \frac{H}{200}$, $c=0.15$, $e= 0.30$ and $f=0.10$ with assuming $d_{50}=0.250$.

Among the equations for predicting the maximum scour depth, which includes an extensive range of laboratory data according to the dimensional analysis, is the relation presented by D'Agostino and Ferro (2004) [10]. Despite the many relations offered after that, it is still one of the most valid relations as Eq. (5).

$$\frac{d_s}{Z_d} = 0.54 \left(\frac{H_t}{H}\right)^{-0.126} (A_{50})^{0.544} \left(\frac{d_{90}}{d_{50}}\right)^{-0.856} \left(\frac{b_s}{B}\right)^{-0.751} \left(\frac{b_s}{Z_d}\right)^{0.593} \quad (5)$$

where $A_{50} = \frac{Q}{b_s Z_d \sqrt{g d_{90} (\Delta - 1)}}$, Q is the flow discharge, B is the channel width, b_s is the width of GCS that may differ from the channel width, and d_{90} is the diameter that 90% of the particles are smaller than it.

One of the newest equations presented to predict d_s and l_s downstream of GCS can be referred to in Eq. (6) and Eq. (7) from Ben Moftah and Mossa (2020) [23]. These equations are presented using a new approach with dimensional analysis.

$$\frac{d_s}{H_c} = 0.24 \left(1 + \frac{Z_d}{H_c} \right)^{0.92} \left(\frac{H_t}{H_c} \right)^{0.24} \left(\frac{\lambda}{\pi} \right)^{-0.34} (Fr_d)^{0.38} \quad (6)$$

$$\frac{l_s}{d_s} = 2.16 \left(\frac{0.22 \left(1 + \frac{Z_d}{H_c} \right)^{0.76} \left(\frac{H_t}{H_c} \right)^{0.68} \left(\frac{\lambda}{\pi} \right)^{-0.16} (Fr_d)^{0.82} (H_c)}{d_s} \right) \quad (7)$$

2.1. Experimental setup

Experimental tests were conducted in a flume with a length of 4 meters, a width of 0.6 meters, and a height of 0.2 meters at the hydraulic lab of Babol Noshirvani University of Technology. This flume was calibrated and used for physical sediment transport in previous studies [25-32]. It includes a channel, upstream and downstream water tank, pump, point gauge, and a gate at the end of the channel to adjust the flow depth (Fig. 1). The flow discharge is controlled by a magnetic flow meter that can supply water up to 0.0083 m³/s. When the pump turns on, the water flows from the upstream tank into the channel and the downstream tank, and then it transfers to the upstream tank through the pipes installed under the channel. This cyclic procedure continues until the pump is on. The point gauge with a resolution of 0.1 mm was used to achieve the flow depths and scour profiles which moved in longitudinal and transverse directions on a metal carriage.

The experimental model of GCS is made of PVC installed at a distance of 0.75 meters from the channel's beginning. GCS includes a sloped surface 0.4 meters long with an angle of 20.5 and a rectangular cube 0.5 meters long, 0.15 meters high, and the width equal to the channel width, with two varied slopes of 90° and 60° at the downstream face. Ben Meftah and Mossa (2020) [23] suggested that to ensure the development of the flow, the GCS experimental model should be installed at a distance of one meter from the beginning of the channel. To provide more suitable development of the flow, and reduce its turbulence, a grid screen was used before the water flow inlet in a channel to calm it down. In tests, the water passed through the grid screen, and after 0.75 m reached the GCS, the flow overflowed on the sedimentary bed, and the scour process started.

The downstream face of GCS was filled with two different sand materials with a height of 11.6 centimeters, which continues to the end of the channel with a constant height. Experiments have been conducted on two sand beds with an average diameter of $d_{50}=0.8$ and $d_{50}=1.6$ mm, and $\rho_s=2650$ kg/m³. To keep these soils safe against washing, at the end of the erodible bed, the end sill is at a height equal to the height of the sedimentary bed. Figure 1 shows the experimental model in the laboratory and a schematic view.

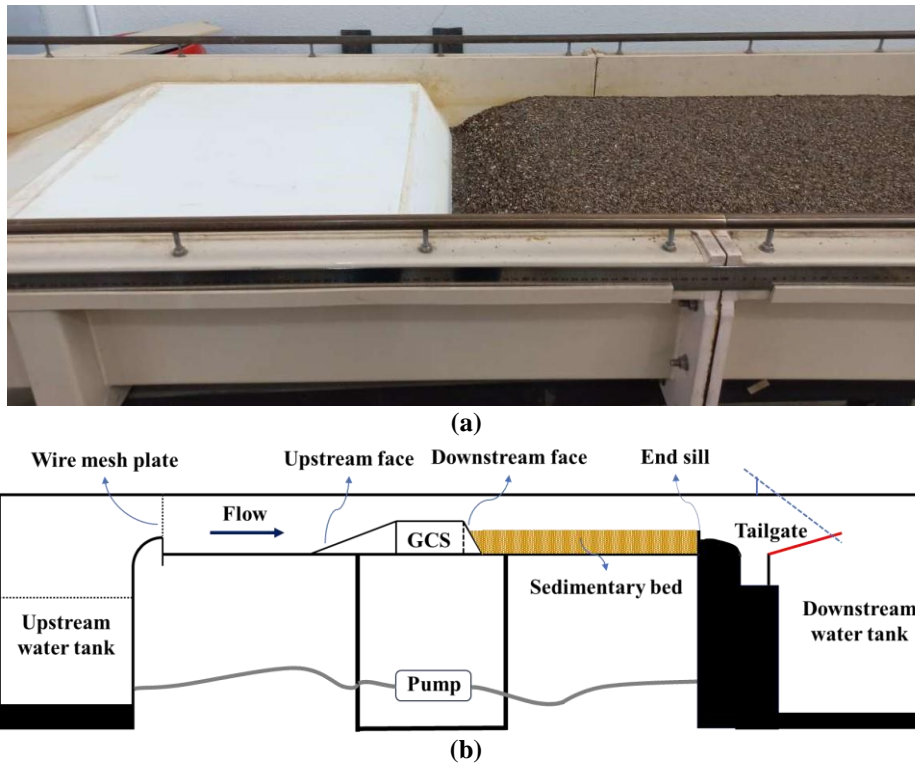


Figure 1. Experimental model in (a) Laboratory (b) Schematic view

The measured values during each test for the scour hole formed downstream of GCS include the maximum equilibrium depth (d_s), the maximum equilibrium length (l_s), the longitudinal profiles of the equilibrium scour hole, critical flow depth (H_c), and tailwater depth (H_t). After finding the location of d_s along the channel's centerline in the longitudinal direction, along the location of d_s , scour depth was measured in the transverse direction of the channel, was to obtain the maximum depth of the final equilibrium scour hole (d_s). Table 1 presents the adjusted values of each test. Experiments were divided into two models based on the grain size of the soil. The first category (model A) consists of soil with $d_{50}=0.82$ mm, and the second (model B) uses soil with $d_{50}=1.6$ mm.

Table 1. Experimental setup of each test

Model	Test	q (m ² /s)	λ (°)	H_t (m)	H_c (m)	d_{50} (mm)
A	A1	0.00467	90	0.018	0.0073	0.82
	A2	0.00583	90	0.020	0.0089	0.82
	A3	0.00700	90	0.023	0.0102	0.82
	A4	0.00467	60	0.018	0.0074	0.82
B	B1	0.00467	90	0.018	0.0077	1.60
	B2	0.00583	90	0.020	0.0105	1.60
	B3	0.00700	90	0.023	0.0091	1.60
	B4	0.00467	60	0.018	0.0070	1.60
	B5	0.00583	60	0.020	0.0081	1.60
	B6	0.00700	60	0.023	0.0092	1.60

3. Results and discussion

3.1. Experimental results

To avoid undesirable initial scour in all tests, in the beginning, each test was started with the lowest flow discharge of 0.0013 m³/s. After the flow passed over the GCS flowed on the sedimentary bed, and reached the end sill, the flow was adjusted to the desired flow discharge. In all tests, the maximum depth of the scour hole downstream of GCS and its maximum length were measured and shown in Table 2.

Table 2. Maximum scour depth and length of each test

Model	Test	Fr _d	d _s (m)	l _s (m)
A	A1	5.55	0.0924	0.290
	A2	5.69	0.1096	0.335
	A3	5.96	0.0740	0.455
	A4	5.47	0.0998	0.270
B	B1	3.77	0.0477	0.205
	B2	3.98	0.0666	0.245
	B3	4.14	0.0369	0.355
	B4	4.14	0.0750	0.190
	B5	4.48	0.0822	0.230
	B6	4.73	0.0898	0.240

One of the most critical issues in the discussion of scour in the laboratory is determining the equilibrium time of the scour process. The equilibrium scour time is when the geometry of the scour hole does not vary after that. In other words, the sediment bed particles are not separated from the scour hole by the water flow. A crucial factor in determining the equilibrium scour time is the type of soil granulation. It is clear that the larger the laboratory scale and the coarser soil granularity, the more time is needed to reach the equilibrium scour hole. In 2018, Wang et al. [33] investigated the bed morphology downstream of GCS with a larger laboratory scale and coarser soil granularity than this research. They considered the equilibrium scour time in their studies to be 120 minutes, and according to their observations, during this time, the scour hole reached an equilibrium state. The equilibrium scour time in Rajaei et al. [13] in 2018 was about 270 minutes. At three times, 5, 30, and 270 minutes, the values of changes in the geometry of the longitudinal scour profile downstream of the GCS were investigated. The ratio of equilibrium time in their research is as follows: $\frac{t}{t_e} = 0.013$ for 5 minutes, $\frac{t}{t_e} = 0.083$ for 60 minutes, and $\frac{t}{t_e} = 0.75$ for 270 minutes. Where t represents time and t_e represents equilibrium time. According to Breusers and Raudkivi [34], sometimes the scour time is so long that it may never be achieved. Of course, sometimes the scour time is so short that it can be less than 60 minutes. For example, Pagliara and Palermo [11] observed that only in 40 minutes, the scour hole reaches its equilibrium state.

There were a lot of disagreements regarding the equilibrium scour time, then a 360-minute test was performed at first. In the first 10 minutes, it was found that the scour hole developed quickly. Then, the expansion rate of the scour hole starts to reduce. At 90 minutes after the start of the scour process, the geometry of the scour hole was very close to its equilibrium state. After about 240 minutes, the sediment bed particles were hardly separated from the water flow from the scour hole and even returned to the hole due to hydraulic jump and backward flow. As a result, 240 minutes was chosen as the final and equilibrium scour time for all experiments.

3.2. Longitudinal profile of scour hole downstream of GCS

The proper process of forming the geometry of the scour hole is fundamental in obtaining d_s and l_s . Several studies, such as Bormann and Julien (1991) [6], Mossa (1998) [7], and Ben Meftah and Mossa (2020) [23], previously showed that the most significant effect on the final geometry of the longitudinal profile of the scour hole depends on the scour process time, flow intensity, depth of tailwater, particle Froude number, type of soil granularity, water drop, flow depth of flow on the end of the GCS crest and the slope of the downstream face of GCS. For example, one of the equations that shows the relationship between these parameters is Eq. (6) and Eq. (7). In most of the experiments of this research, the longitudinal profile of the equilibrium scour hole was spoon-shaped. Figure 2 presents the longitudinal patterns of the scour hole in the equilibrium state for tests A1, A2, B1, and B2.

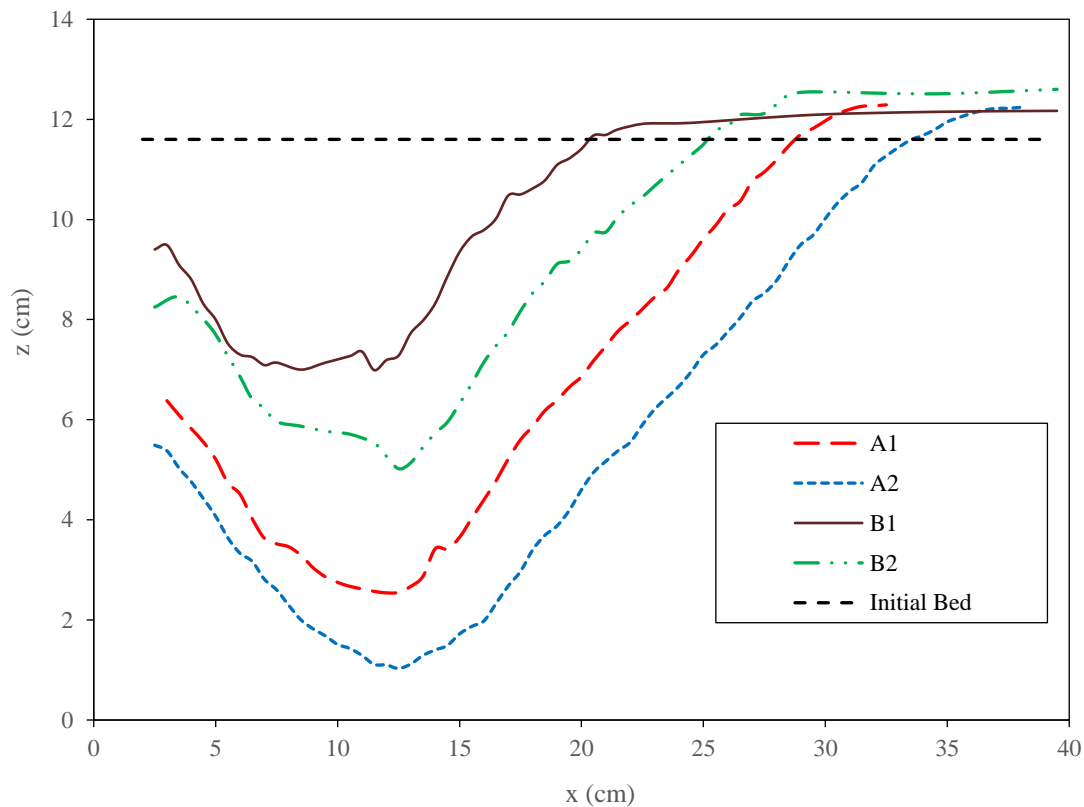


Figure 2. Longitudinal profile of the scour hole in tests A1, A2, B1, and B2

3.3. Influence of sediment size on d_s and l_s

Experimental observations indicated that under the constant flow discharge and geometry of GCS and different soil granularity, the maximum length and depth of the scour hole decreased by increasing the sediment size. As shown in Table 2, increasing the flow discharge in both types of soil, increases l_s . Figure 3 compares d_s and l_s downstream of the vertical GCS in different sediment sizes.

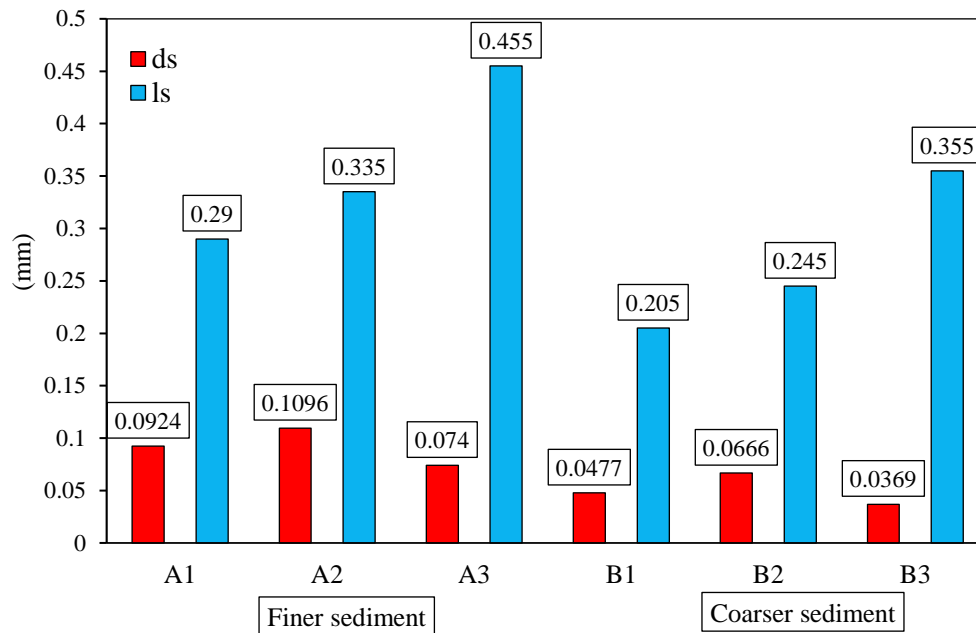


Figure 3. Comparison of d_s and l_s downstream of the vertical GCS with different sediment sizes

Although in tests A3 and B3, $q=0.007 \text{ m}^2/\text{s}$ (more than in other tests), d_s in test A3 is lower than A1 and A2, as well as d_s in test B3 was lower than in tests B2 and B3. This result occurs because in this case, the Froude number is higher than one, which leads to the formation of hydraulic jump and return flow. The hydraulic jump is often formed on the scour hole near the bed sediment. Already, Chanson [35] has mentioned this issue. This phenomenon, a type of reverse flow, leads to the return of sediment particles into the scour hole. Figure 4 shows the hydraulic jump formed downstream of GCS with the vertical face on the scour hole.



Figure 4. Hydraulic jump formed downstream of GCS

As mentioned in the technical literature, increasing the flow velocity leads to more erosion of the sedimentary bed. In all tests, it was observed that the increase in the flow discharge increased l_s . The accuracy of this conclusion has already been declared in the study of Ben Meftah and Mossa (2020) [23].

3.4. Influence of the slope of GCS downstream face on d_s and l_s

The comparison between vertical and inclined GCS has already been studied, such as Bormann and Julien (1991) [6] and Ben Meftah and Mossa (2020) [23]. These studies indicated that under the same hydraulic conditions, d_s and l_s changed with the variations of the slope of the downstream face of GCS. As the slope decreases from 90° in different hydraulic conditions, d_s , and l_s increase or decrease. In this research, in the sedimentary bed with $d_{50}=1.6$ mm, under constant hydraulic conditions, d_s downstream of GCS with an angle of 60° is more than 90° , in comparison l_s downstream of GCS with the face of 60° became less than 90° . Figure 5 indicates d_s and l_s downstream of the vertical and inclined GCS in the constant sediment sizes.

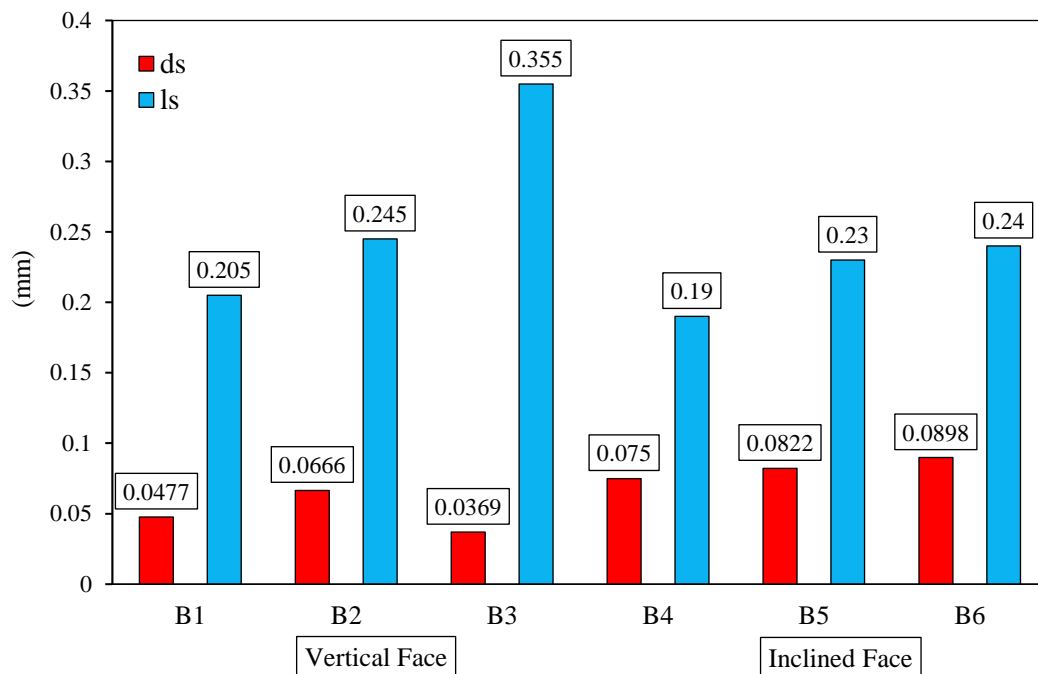


Figure 5. Comparison of d_s and l_s downstream of the inclined and vertical GCS with the constant sediment sizes

Test A4 was performed under $q=0.004667$ m²/s, $\lambda=60^\circ$ and $d_{50}=0.82$ mm. Although this test was conducted in the same sedimentary conditions and different geometrical conditions from test A1, in terms of the geometry of GCS it was similar to test B1 and different in terms of sediment sizes. For this reason, the data obtained from test A4 are compared and analyzed with tests A1 and B1, respectively. Investigations showed that although d_s in test A4 was greater than in test A1, l_s was reduced. It can be concluded that under the same sedimentary condition, by decreasing the slope of the GCS downstream face from 90° to 60° , d_s increases, and l_s decreases. Also, in similar geometrical conditions, i.e. downstream face of 60° degrees and different sedimentary conditions, as expected, the coarser sediment, d_s , and l_s decreases.

3.5. Discussion

Accurate prediction of the d_s is always one of the biggest problems in river engineering. In the meantime, researchers presented a series of predictive experimental equations previously mentioned in the technical literature. The data collected from d_s in the present study is displayed in a dimensionless form in Table 3.

Table 3. The dimensionless values of d_s/H_c based on Fr_d changes

Model	Test	Fr_d	d_s/H_c
A	A1	5.55	12.66
	A2	5.69	12.31
	A3	5.96	7.25
	A4	5.47	13.49
B	B1	3.77	6.19
	B2	3.98	7.32
	B3	4.14	3.51
	B4	4.14	10.71
	B5	4.48	10.15
	B6	4.73	9.76

In Figure 6, d_s/H_c was compared between the present study and Ben Meftah and Mossa (2020) [23]. Statistical index calculations revealed a correlation coefficient ($R^2=0.891$) and relative error ($RE\%=10.66\%$). These values present acceptable differences between the present study results and previous data.

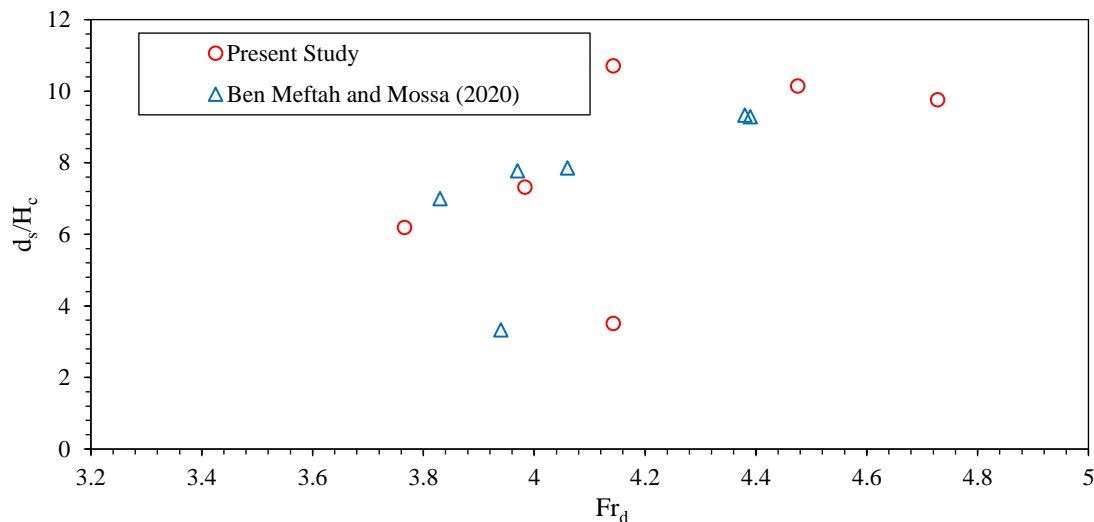


Figure 6. Comparison of d_s/H_c between the present study and Ben Meftah and Mossa (2020)

In the same geometric conditions of the experimental model, it was observed that for finer sediments, the maximum length and depth of the scour hole increases compared to the coarser sediment condition. This is obvious because, in finer sediment conditions, sediment particles could be moved up more easily. The settling velocity of sediment is a function of particle diameter. In larger particles, the rate of sedimentation will increase. Chanson [35] mentioned that bed-load transport occurs when the bed shear stress is larger than a critical value.

In the constant sedimentary conditions and different GCS geometries, it was observed for GCS with the downstream vertical face, d_s decreases, and by changing the slope from 90° to 60° , d_s increases. In reverse, l_s in GCS with a slope of 60° reduced compared to GCS with a slope of 90° . It can be concluded that in the vertical slope, the longitudinal profile of the scour hole is stretched along the longitudinal axis, and its depth is reduced. Results of tests A3 and B3 indicated that despite the highest discharge, the maximum scour depth became less. This result was obtained due to the formation of anti-dune downstream of GCS in these cases.

4. Conclusion

Grade control structures (GCS) are countermeasures to reduce river erosion. Since scouring downstream of these structures leads to their failure and damage, it is necessary to study scouring downstream of GCS. This research investigated the downstream morphology of GCS with inclined and vertical downstream faces in the river under different hydraulic and sedimentary beds, and the effect of each effective parameter was evaluated. It was shown that in the same GCS geometry and finer-grained sedimentary conditions, the values of scouring were larger than in coarser-grained conditions. This is obvious because, in finer-grained conditions, it is more possible for particles to be suspended and moved with water flow. A comparison was made in the same sediment conditions and different geometries, and the results showed that when the downstream face of GCS is vertical, d_s is less than when it is inclined. While the maximum scour lengths obtained in vertical faces were more than in inclined conditions. It was also concluded that the hydraulic jump significantly influences the final geometry of the equilibrium scour hole due to the returning flow it creates. Although the flow discharges were highest in some tests, the maximum scour depth was lower, and an antidune was formed downstream of GCS because the Froude number became higher than 1. It was concluded that in the same sediment conditions, by reducing the slope of the downstream face of GCS from 90° to 60° , d_s increases, and l_s decreases. Also, in the same geometry and different sediments, in coarser-grained conditions, the values of scour decreases. The results of this study could be used as a small-scale experimental model to distinguish the geometry of GCS on scour parameters, but flow characteristics in scour holes were not investigated. It is recommended to conduct other studies to evaluate the influence of the secondary current on the location of the maximum depth of the scour hole. Also, the effect of the roughness of GCS on the scour hole profiles and flow characteristics can be investigated.

Acknowledgements

The authors appreciate Mr. Ali Mahdian Khalili, the executive officer and senior researcher of the hydraulic lab at Babol Noshirvani University of Technology, for his worthy help in performing this research.

References

1. Mahdian Khalili A, Hamidi M, (2023). Time evolution effect on the scour characteristics downstream of the sluice gate with the submerged hydraulic jump in a laboratory model. *Journal of Hydraulic Structures* 9(2), pp: 32-47. <https://doi.org/10.22055/JHS.2023.43499.1249>.
2. Sattar AM, Plesiński K, Radecki-Pawlik A, Gharabaghi B. (2018). Scour depth model for grade-control structures. *Journal of Hydroinformatics* 20(1), pp: 117-133. <https://doi.org/10.2166/hydro.2017.149>
3. Korpak J, Lenar-Matyas A, Radecki-Pawlik A, Plesiński K, (2021). Erosion irregularities resulting from series of grade control structures: The Mszanka River, Western Carpathians. *Science of The Total Environment* 799, 149469. <https://doi.org/10.1016/j.scitotenv.2021.149469>
4. Khalili AM, Hamidi M, Dadamahalleh PA, (2023). Introducing Countermeasures for Reducing Bed Scour of Mountainous Rivers, 1st International Conference on Sustainable Mountain, 11&12 December 2023, University of Mohaghegh Ardabili.
5. Shafai-Bejestan M, Nabavi SMR, Dey S, (2016). Scour downstream of grade control structures under the influence of upward seepage. *Acta Geophysica*, 64, pp: 694-710. <https://doi.org/10.1515/acgeo-2016-0024>
6. Bormann NE, Julien PY, (1991). Scour downstream of grade-control structures. *Journal of Hydraulic Engineering* 117(5), pp: 579-594. [https://doi.org/10.1061/\(ASCE\)0733-9429\(1991\)117:5\(579\)](https://doi.org/10.1061/(ASCE)0733-9429(1991)117:5(579))
7. Mossa M, (1998). Experimental study on the scour downstream of grade-control structures. *Proc., 26th Convegno di Idraulica e Costruzioni Idrauliche*, pp: 581-594.
8. Lenzi MA, Marion A, Comiti F, (2003). Local scouring at grade-control structures in alluvial mountain rivers. *Water Resources Research* 39(7). <https://doi.org/10.1029/2002WR001815>
9. Marion A, Lenzi MA, Comiti F, (2004). Effect of sill spacing and sediment size grading on scouring at grade-control structures. *Earth Surface Processes and Landforms: The Journal of the British Geomorphological Research Group*, 29(8), pp: 983-993. <https://doi.org/10.1002/esp.1081>
10. D'Agostino V, Ferro V, (2004). Scour on alluvial bed downstream of grade-control structures. *Journal of Hydraulic Engineering* 130(1), pp: 24-37. [https://doi.org/10.1061/\(ASCE\)0733-9429\(2004\)130:1\(24\)](https://doi.org/10.1061/(ASCE)0733-9429(2004)130:1(24))
11. Pagliara, S., & Palermo, M. (2013). Rock grade control structures and stepped gabion weirs: Scour analysis and flow features. *Acta Geophysica* 61, pp: 126-150. <https://doi.org/10.2478/s11600-012-0066-0>
12. Pagliara S, Kurdistani SM, (2014). Scour characteristics downstream of grade-control structures. *River flow 2014*, pp: 2093-2098.
13. Rajaei A, Esmaeili Varaki M, Shafei Sabet B, (2020). Experimental investigation on local scour at the downstream of grade control structures with labyrinth planform. *ISH Journal of Hydraulic Engineering* 26(4), pp: 457-467. <https://doi.org/10.1080/09715010.2018.1502627>
14. Di Nardi J, Palermo M, Bombardelli FA, Pagliara S, (2021). The phenomenological theory of turbulence and the scour evolution downstream of grade-control structures under steady discharges. *Water* 13(17), 2359. <https://doi.org/10.3390/w13172359>
15. Sohrabzadeh H, Ghodsian M, (2022). Experimental study of the effect of sidewall slope over the triangular PK weir. *Journal of Hydraulics*, 17(4), 17-30. <https://doi.org/10.30482/JHYD.2022.326177.1581>

16. Sohrabzadeh Anzani H, Ghodsian M, (2024). Experimental study of flow over piano key weirs with different plan shapes. *ISH Journal of Hydraulic Engineering* 30(2), 185-195. <https://doi.org/10.1080/09715010.2024.2302808>
17. Lantz WD, Crookston BM, Palermo M, (2022). Evolution of local scour downstream of Type A PK weir in non-cohesive sediments. *Journal of Hydrology and Hydromechanics* 70(1), pp: 103-113. <https://doi.org/10.2478/johh-2021-0035>
18. Khalili AM, Hamidi M, (2023). Experimental investigation of submerged hydraulic jump downstream of sluice gate in erodible channel. *Proc. of the 13th International Congress on Civil Engineering*, Tehran.
19. Guguloth S, Pandey M, (2023). Accuracy evaluation of scour depth equations under the submerged vertical jet. *AQUA—Water Infrastructure, Ecosystems and Society* 72(4), pp: 557-575. <https://doi.org/10.2166/aqua.2023.015>
20. Guguloth S, Pandey M, Pal, (2024). Application of Hybrid AI Models for Accurate Prediction of Scour Depths under Submerged Circular Vertical Jet. *Journal of Hydrologic Engineering* 29(3), 04024010. <https://doi.org/10.1061/JHYEFF.HEENG-6149>
21. Ben Meftah M, De Padova D, De Serio F, Mossa M, (2021). Secondary currents with scour hole at grade control structures. *Water* 13(3), 319. <https://doi.org/10.3390/w13030319>
22. Noormohammadi G, Esmaeili Varaki M, Radice A, Shafiee Sabet B, (2018). Experimental Investigation on Local Scour at Downstream of the Inclined Grade Control Structure. *Irrigation and Drainage Structures Engineering Research* 19(72), pp: 51-68. <https://doi.org/10.22092/idser.2017.114767.1239>
23. Ben Meftah M, Mossa M, (2020). New approach to predicting local scour downstream of grade-control structure. *Journal of Hydraulic Engineering* 146(2), 04019058. [https://doi.org/10.1061/\(ASCE\)HY.1943-7900.0001649](https://doi.org/10.1061/(ASCE)HY.1943-7900.0001649)
24. Mason PJ, Arumugam K, (1985). Free jet scour below dams and flip buckets. *Journal of Hydraulic Engineering* 111(2), pp: 220-235. [https://doi.org/10.1061/\(ASCE\)0733-9429\(1985\)111:2\(220\)](https://doi.org/10.1061/(ASCE)0733-9429(1985)111:2(220))
25. Koohsari A, Hamidi M, (2021). Experimental study of the effect of mining materials downstream of bridge pier on scour profile with optimizing distance approach. *Journal of Water and Soil Conservations*, 28(3), pp: 1-26. <https://doi.org/10.22069/JWSC.2022.19400.3490>
26. Akbari Dadamahalleh P, Hamidi M, Mahdian Khalili A, (2022). Experimental Prediction of the Bed Profile with the Full-submerged and Semi-submerged Debris Accumulation Upstream of the Cylindrical Bridge Pier. *Journal of Water and Soil Conservation*, 29(4), pp: 95-114. <https://doi.org/10.22069/JWSC.2023.20642.3582>.
27. Mahdian Khalili A, Hamidi M, Akbari Dadamahalleh P, (2023). Scour Morphology around the Bridge Pier with Upstream Rectangular Debris. 22nd Iranian Conference on Hydraulics, 8-9 November 2023, University of Maragheh.
28. Hamidi M, Sadeqlu M, Khalili AM, (2024). Investigating the design and arrangement of dual submerged vanes as mitigation countermeasure of bridge pier scour depth using a numerical approach. *Ocean Engineering* 299, 117270. <https://doi.org/10.1016/j.oceaneng.2024.117270>
29. Mahdian Khalili A, Akbari Dadamahalleh P, Hamidi M, (2024). Experimental evaluation of dune formation downstream of pier scour hole with upstream debris accumulation. *Journal of Hydraulic Structures* 10(1), pp: 13-28. <https://doi.org/10.22055/JHS.2024.45772.1281>
30. Dadamahalleh PA, Hamidi M, Khalili AM (2024) Bed sill effect on bridge pier scour with debris obstruction: an experimental investigation. *Innovative Infrastructure Solutions* 9(5),

- pp: 142. <https://doi.org/10.1007/s41062-024-01447-z>
31. Khalili AM, Hamidi M, Dadamahalleh, PA (2024). Experimental study of the effect of rectangular debris blockage on the scour hole development around a cylindrical bridge pier. *Water Practice & Technology* 19(5), pp: 1878-1892. <https://doi.org/10.2166/wpt.2024.092>
 32. Hamidi M, Koohsari A, Khalili AM (2024). Numerical investigation of mining pit effects on maximum scour depth around bridge pier with different shape. *Modeling Earth Systems and Environment*, 1-15. <https://doi.org/10.1007/s40808-024-02057-5>
 33. Wang JM, Yang XG, Zhou HW, Lin X, Jiang R, Lv EQ, (2018). Bed Morphology around various solid and flexible grade control structures in an unstable gravel-bed river. *Water* 10(7), 822. <https://doi.org/10.3390/w10070822>
 34. Breusers NHC, Raudkivi AJ, (1991). *Hydraulic structure design manual: scouring*. IAHR design manual, 2.
 35. Chanson H, (2004). *Hydraulics of open channel flow*. Elsevier.



© 2024 by the authors. Licensee SCU, Ahvaz, Iran. This article is an open access article distributed under the terms and conditions of the Creative Commons Attribution 4.0 International (CC BY 4.0 license) (<http://creativecommons.org/licenses/by/4.0/>).

